Thermo-Electrical Analysis of an Anode Design

Tuofu Li[1], Hicham Chaouki[2], Wenju Tao[3], Jianfeng Hou[4], Zhaowen Wang[5] and Mario Fafard[6]

1. Ph.D. student
3. Postdoctor
4. Ph.D. student,
5. Professor

School of Metallurgy, Northeastern University, Shenyang, 110819, China

1. Ph.D. student,
2. Research assistant
6. Professor

NSERC/Alcoa Industrial Research Chair MACE^3 and Aluminium Research Centre—REGAL, Laval University, Quebec City, QC G1V 0A6, Canada

Corresponding author: tuofuli@hotmail.com

Abstract

Anode design has significant effects on power saving of aluminium production. In this paper, the effects of an existing anode design on anode voltage drop have been investigated using thermo-electrical analysis. In this design, used currently in some Chinese smelters, a pin was added in the bottom of the centre of the stub hole. This part, originally designed for rodding process, could help to reduce the anode total voltage drop through improving the electrical contact resistance between cast iron thimble and carbon. For this purpose, a thermo-electrical model was developed using ANSYS software and different contact scenarios were taken into account in order to estimate the anode total voltage drop reduction. Simulation results show that this design leads to a non-negligible voltage drop reduction ranges from 2.3 to 5.6 mV, which can bring electrical cost saving from 145 792 $ to 353 206 $ per year for a smelter producing approximately 500 kt/y of aluminium, if the energy cost is 40 $/MWh.

Keywords: Aluminium production, anode design, anode voltage drop, thermo-electrical analysis.

1. Introduction

Primary aluminium production is a high-energy consumption process. The power consumed is about 13.0 kWh/kg Al, but the electric energy efficiency is only about 50 %. What's more, the CO_2 emission due to the aluminium production is also a problem. In modern aluminium reduction process, the anode voltage drop is over 300 mV, according for 7.5 % of the total voltage drop [1]. Therefore, the optimization of the anode design is of great interest and could help to reduce the power consumption of Hall-Héroult process.

Researchers have tried different designs to reduce the anode voltage drop, especially the stub to

carbon contact voltage drop. Tsomaev [2] proposed an anode design which uses a mechanical assemble instead of pouring cast iron in stub hole. The “stub” has a bigger head on its end, and the anode has a slot with the same shape (Figure 1). Its advantage is that there would not be air gap without cast iron. What’s more, the contact area increased. However, this one is difficult to maintain if the “stub” deforms with time.

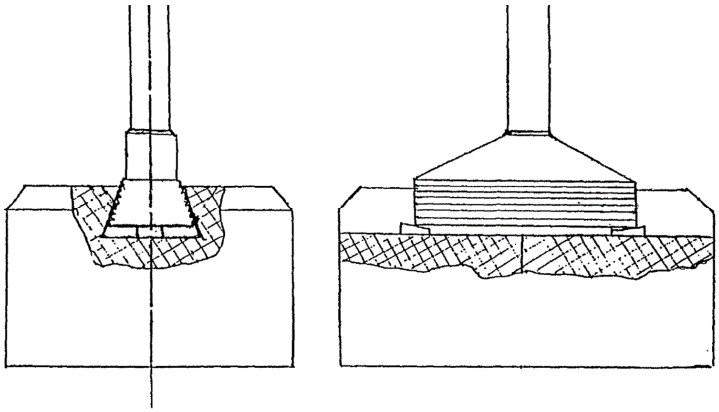

Figure 1. The stub proposed by Tsomaev [2].

Fafard et al. [3] has also published a patent about a new kind of anode connection method, as shown in the Figure 2. There is a slot on the top of the carbon block where the stub can be put into it. This design can increase the contact area between the cast iron and the carbon which will lead to a reduction of the electrical contact resistance. However, the rodding process would be very complicated due to the geometry of the stub.

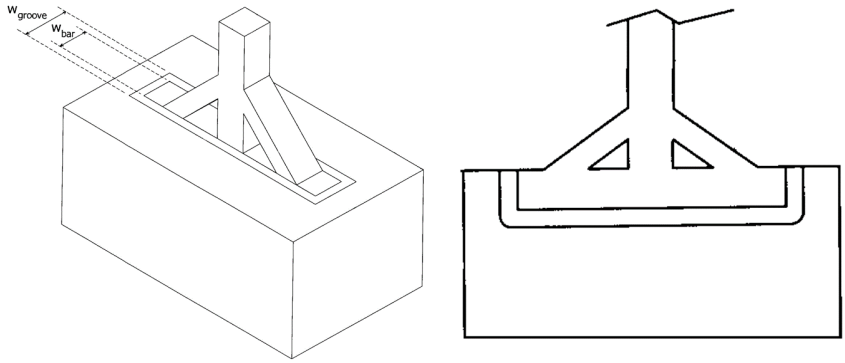

Figure 2. The anode proposed by Fafard et al. [3].

Tremblay et al. [4] also proposed a new anode design where only one stub hole is used and metal components were incorporated in the anode as shown in Figure 3. During the anode baking process, metal connectors are sealed to the carbon block with such a design it is expected that the air gap induced by the shrinkage of cast iron will be reduced. Furthermore, it can lead to a reduction of the electrical contact resistance. Nevertheless, the effect of metal components on the anode behavior, especially clearing the baking process, has to be investigated.

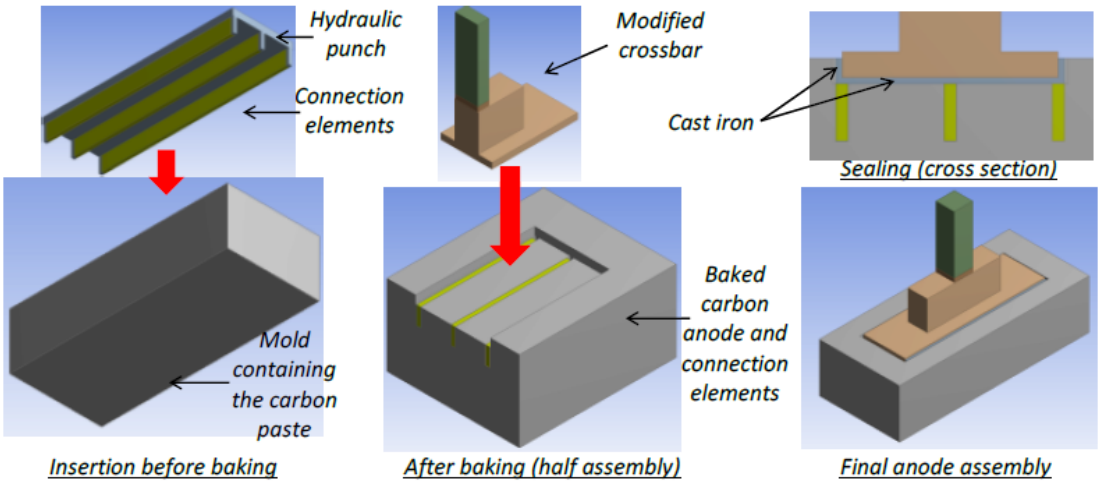

Figure 3. The anode proposed by Tremblay [4].

Hongjun Zhao [5] proposed a new design with each two adjacent stub holes connecting by a slot, as Figure 4. This design can increase the contact area and improve the stub deformation. An industrial measurement indicates that it can bring a voltage drop saving of 20 – 40 mV.

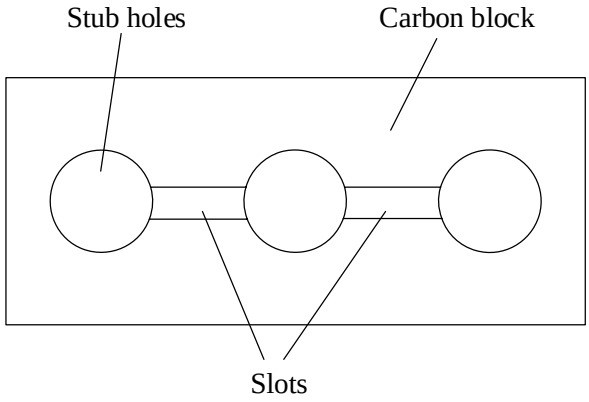

Figure 4. Schematic picture of the anode proposed by Hongjun Zhao.

In a recent Chinese patent [6], a pin was added at each bottom of the stub hole, as shown in Figure 5. The pin was originally designed to make the liquid cast iron flow evenly in order to reduce defects in cast iron thimbles. Despite the simplicity of this design, it is expected that it could improve electrical contact resistance.

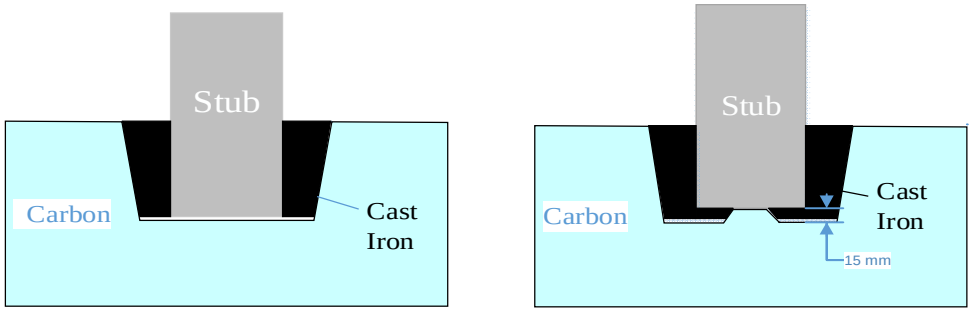

Figure 5. Conventional anode design (left) and the anode design in the patent (right).

The 3-D geometry of cast iron thimble (Figure 6a) and the section of stub hole (Figure 6b) are illustrated. Figure 6b illustrates that this design can bring two potential contact interfaces compared with the normal anode. The increased contact interfaces would lead to a reduction of the contact voltage drop.

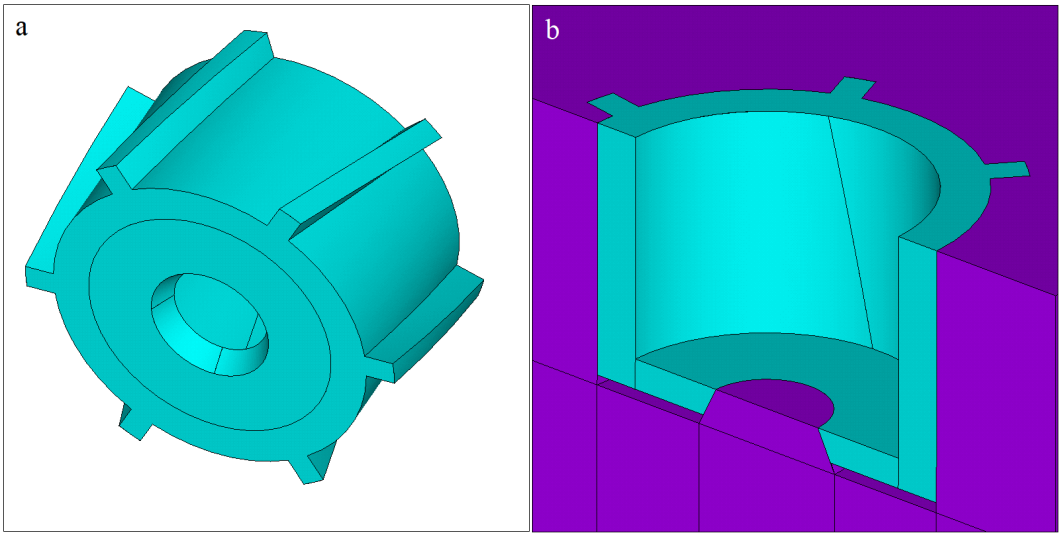

Figure 6. 3-D geometry of cast iron thimble and section of the stub hole.

The aim of this work is to investigate the effect of such a design on the anode behavior. For this purpose, a thermo-electrical model was developed using the APDL language of ANSYS software. Several contact cases were considered in order to estimate the potential of this design.

2. Model and description

The model consists of an assembly containing the anode, cast iron thimbles, steel stubs, the aluminium rod and the crossbar (Figure 7).

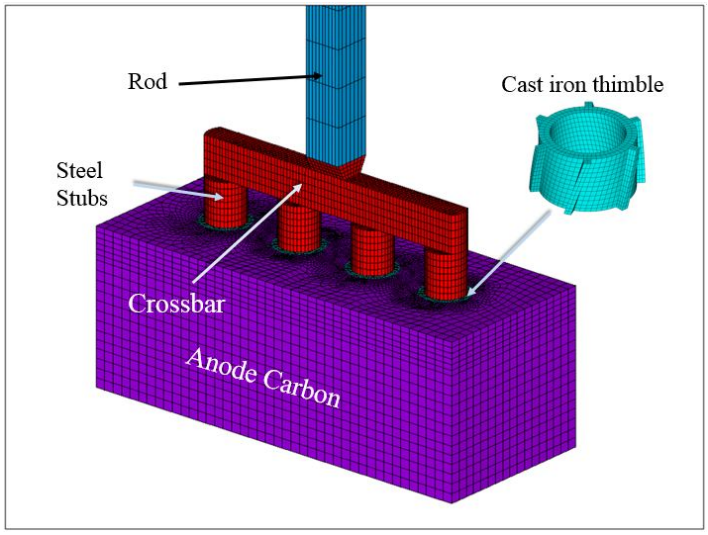

Figure 7. The finite element model.

The anode design is based on 4 stubs, having 6 flutes for each stub holes as shown in Figure 8a. The air gap between the bottom of cast iron thimble and the stub hole is equal to 2 mm. The solid 69 element was used to take into account the thermo-electrical behavior, while contact 173 and Target 170 elements were used to handle contact issues. Figure 8b shows the contact elements between cast iron thimble and the stub hole. The main dimensions of the model are depicted in Table 1.

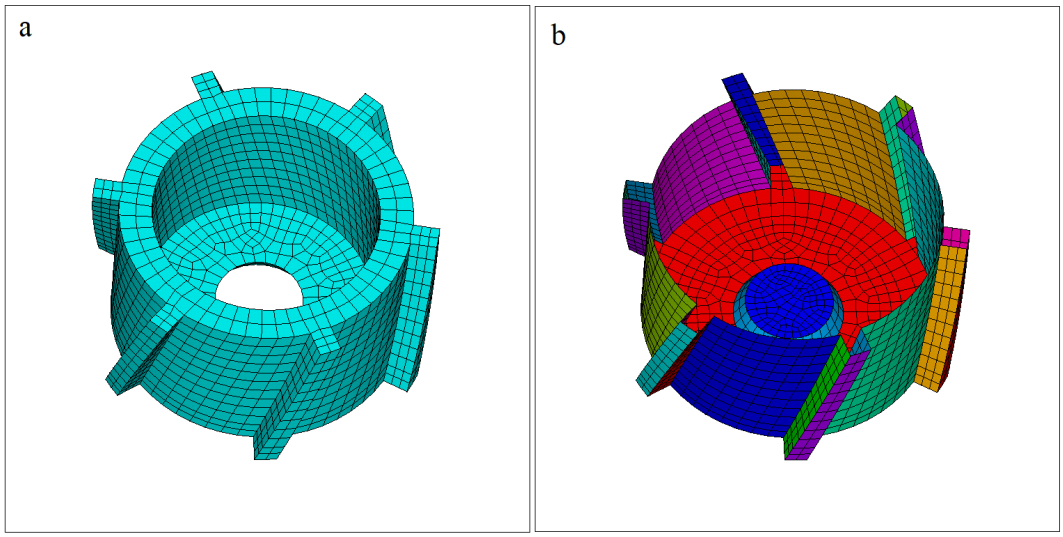

Figure 8. Finite element model of cast iron and the contact elements.

Table 1. Main dimensions of the model.

Component	Dimension（mm）	Component	Dimension（mm）
Carbon block	1650 × 680 × 620	Stub hole diameter	200
Stub diameter	155	Anode rod length	1500
Stub hole depth	115	Anode rod section	150 × 150

There are 4 materials in the model, including the carbon, cast iron, steel and aluminium. The physical properties of different materials, such as thermal conductivity and the electrical resistivity, were taken from the literature [7].

The electrical contact resistance at the cast iron/carbon interface corresponds to the constitutive law proposed by Richard et al [8], which takes into account the mechanical pressure and the temperature evolution. Since in the present study the mechanical behavior is not taken into account, the electrical contact resistance was defined for a mechanical pressure equal to 5 MPa.

For the thermal contact conductance at the cast iron/carbon interface the model proposed in [9] was adopted. In the bottom part of the stub hole, contact thermal conductance is 100 W/m^2K considering the air gap between the bottom of stub and stub hole is specified to be 2 mm, while the contact thermal conductance is 250 W/m^2K in the wall of the stub hole.

The applied boundary conditions are illustrated in Figure 9 and the thermal boundary conditions are summarized in Table 2. On the top of the aluminium rod an electrical current of 10 kA was applied, which corresponds to a total current of 400 kA applied on cell containing 40 anodes. At the bottom of the anode, the voltage drop is set to 0 V. Thermal boundary conditions were taken from [10].

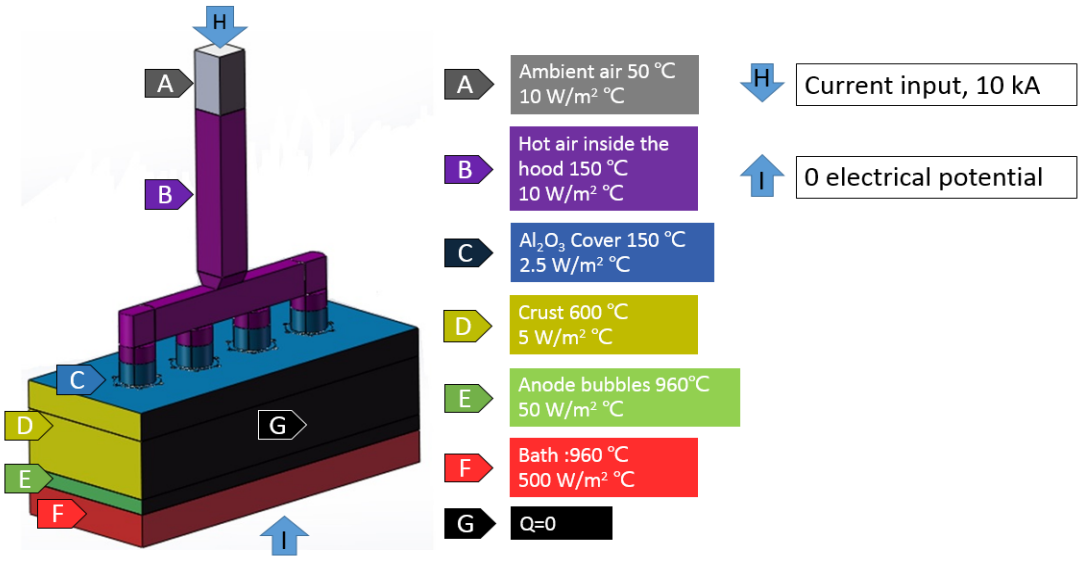

Figure 9. Boundary conditions.

Table 2. Thermal boundary conditions.

Label	Component	Ambient temperature (°C)	Heat transfer coefficient (W/m^{2}K)
A	Ambient air	50	10
B	Hot air inside the hood	150	10
C	Alumina Cover	150	2.5
D	Crust	600	5
E	Anode bubbles	960	50
F	Bath (150 mm)	960	500
G	Anode	-	-

3. Simulation Results

In order to assess predictive capabilities of the studied design, finite element simulations were carried out. In a first step, a conventional design, without the pin was simulated. In a second step, the new design, with several cases for the different contact status at cast iron/pin interface, was simulated.

3.1. Case 1

In this case, results for the conventional design, without the pin, are presented. The contact status between cast iron thimbles and stub holes is shown in Figure 10. Positions under the red lines are the parts in contact. In this case the contact area is approximately 0.42696 m^2.

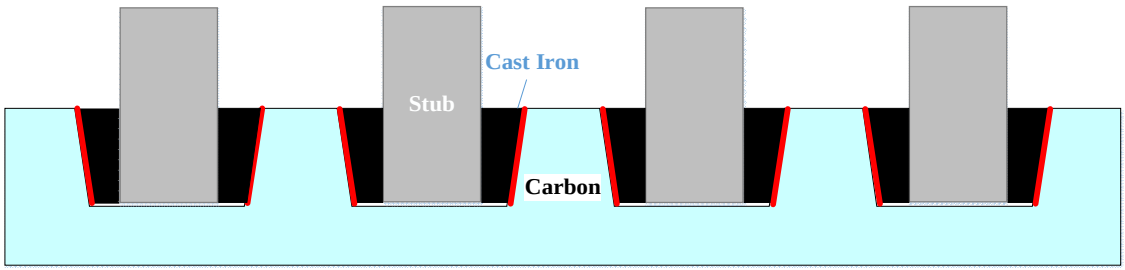

Figure 10. Schematic diagram of contact status in the stub hole.

The voltage drop and the temperature profile are shown in Figure 11. The temperature profile seems to be in agreement with several results found in the literature [8, 9].

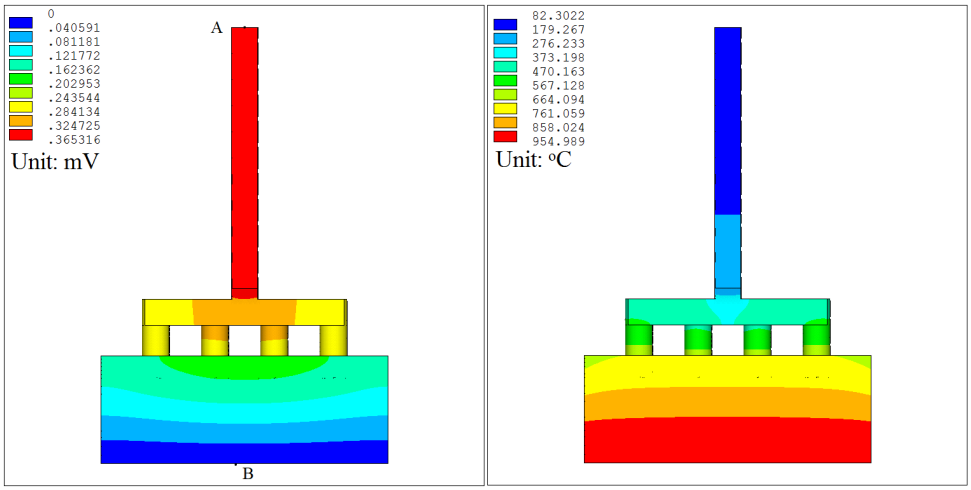

Figure 11. Thermo-electrical results of the conventional anode.

The anode voltage drop, from the rod top to the carbon block bottom, is 365.3 mV. This result is compared with different published results in the literature, which show that it is in a reasonable range (Table 3).

Table 3. Anode voltage drop for different current input values.

	Mohamed I Hassan [11]	Case 1	Hugues Fortin [10]	Daniel Richard [8]	D.D. Gunasegaram [9]
TVD [mV]	379	365	317	307	297
Current input [kA]	11	10	8.25	8.25	7.25

3.2. Case 2

In all subsequent cases, the pin, characterizing the new design, is considered. The ideal situation is that all the contact interfaces keep in contact with each other. As shown in Figure 12, pins contact with the cast iron and the stub respectively. The positions highlighted in red lines are the contact positions. Each pin can bring 2 pairs of contact interfaces, so there are 8 more pairs of contact interfaces in total. The contact surface area increases by about 6 %, to 0.45249 m^2.

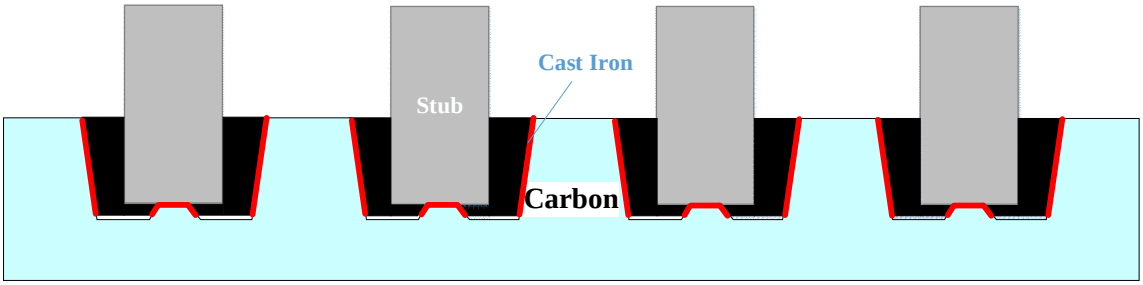

Figure 12. Schematic diagram of contact status in the stub hole of Case 1.

The thermo-electrical results are shown in Figure 13. It is shown that the total anode voltage drop is 359.7 mV. Therefore, if the pins can develop contact with cast iron thimbles and stubs, this design can save for 5.6 mV, which is non-negligible.

However, there is probably some parts in the stub hole which would not keep in contact. Thus, in the following cases, different contact scenarios are simulated. The reason for doing these cases is to simulate the effects of the mechanical field to some extent because the mechanical behavior can make some of the contact interfaces separated. There are three main factors derived from the mechanical field that can affect the contact status, including the gravity, toe-in effect and thermal expansion.

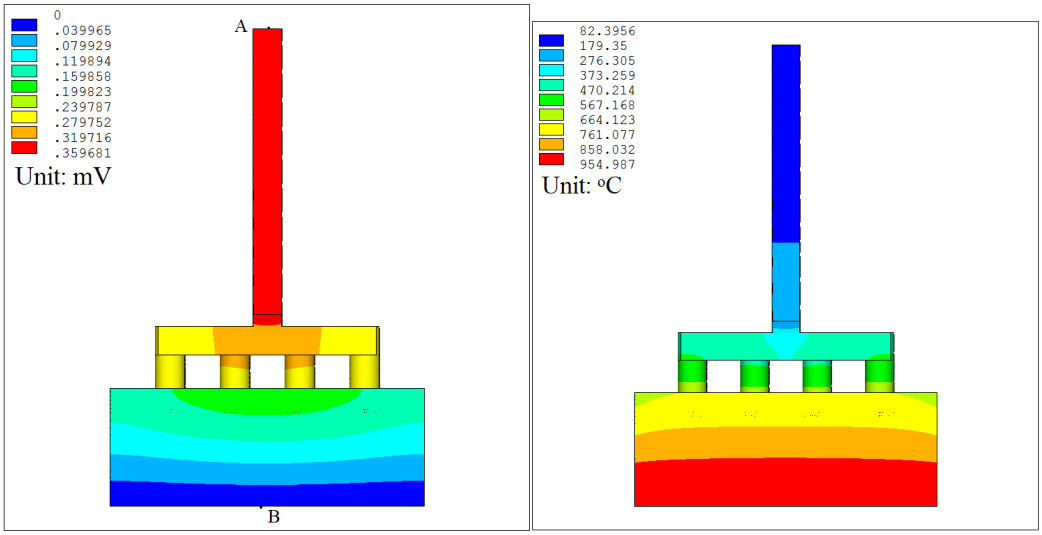

Figure 13. Thermo-electrical results of Case 2.

3.3. Case 3

As known, cast iron would shrink on the stub once solidification takes place and there would be air gap between cast iron and the carbon block. Because of the presence of the airgap, there would be a relative displacement in vertical direction between the cast iron thimble and the stub hole under the gravity force, which would result in a separation of the top surfaces of the pins with the stub bottom. In this case, the top surfaces of the pins are specified to have no contact with the stub bottom. As shown in the Figure 14, the places under red lines are the contact positions, while those under blue lines are not in contact.

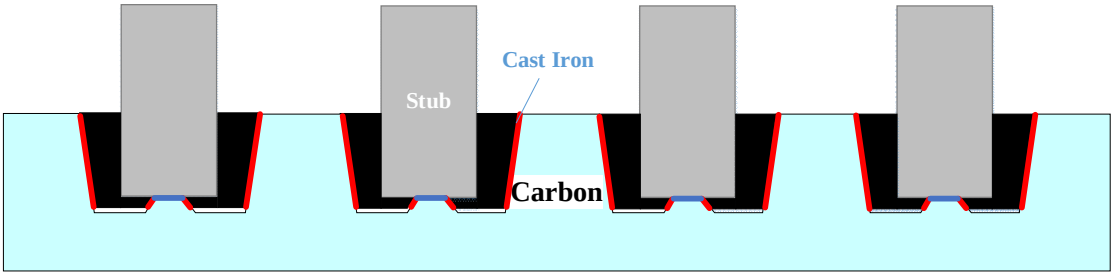

Figure 14. Schematic diagram of contact status in the stub hole of Case 3.

Compared with the conventional anode (Case 1), the contact area in this case increased by about 3.3 %, to 0.44119 m^2. The total anode voltage drop is 361.9 mV. It can save the voltage drop about 3.4 mV compared with Case 1.

3.4. Case 4

Because of the mismatch of the thermal coefficient between the carbon materials and the steel stubs, stub holes constrain the thermal expansion of stubs. So, the heated anode would lead to a toe-in effect which making the outer two stubs bend towards inside which will lead to a contact with the pin top, while the middle two will not. The lateral surfaces of pins are supposed in contact with cast iron thimbles. As shown in Figure 15, the places under red lines are the contact positions, while those under blue lines are not in contact.

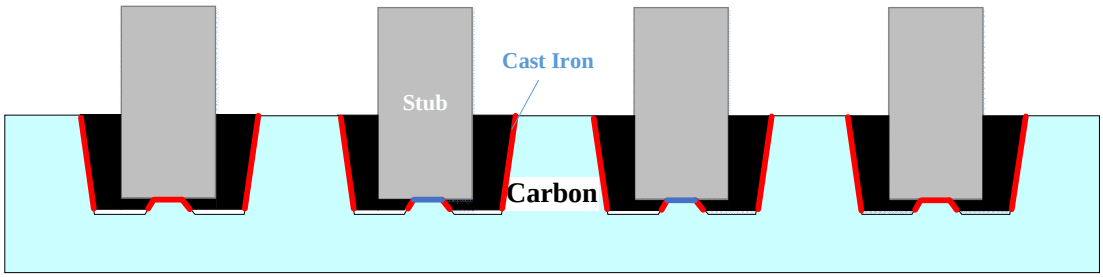

Figure 15. Schematic diagram of contact status in the stub hole of Case 4.

Compared with the conventional anode (Case 1), the contact interfaces area increased by 4.7 %, to 0.44684 m^2. The total anode voltage drop is 360.6 mV here. It can save the voltage drop about 4.7 mV, compared with Case 1.

3.5. Case 5

In this case, the side walls of the pins are not in contact with the cast iron thimbles. As shown in the Figure 16, the places under red lines are the contact positions, while those under blue lines are not in contact.

Compared with the conventional anode (Case 1), the contact area in Case 4 increases only by about 2.6 %, to 0.43827 m^2. However, in this case the anode voltage drop is 360.6 mV, which reduces the voltage drop by 4.7 mV compared to the reference case (Case 1). It is slightly larger

than in Case 4.

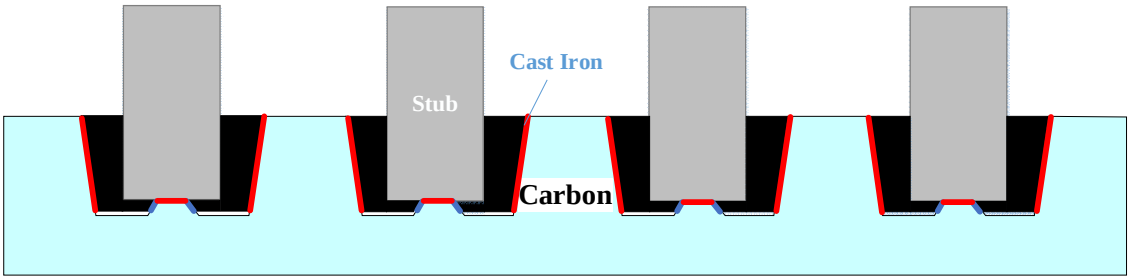

Figure 16. Schematic diagram of contact status in the stub hole of Case 5.

3.6. Case 6

In this case, only the outer two pins contact with the stub bottom on its top surface. As shown in the Figure 17, the places under red lines are the contact positions, while those under blue lines are not in contact.

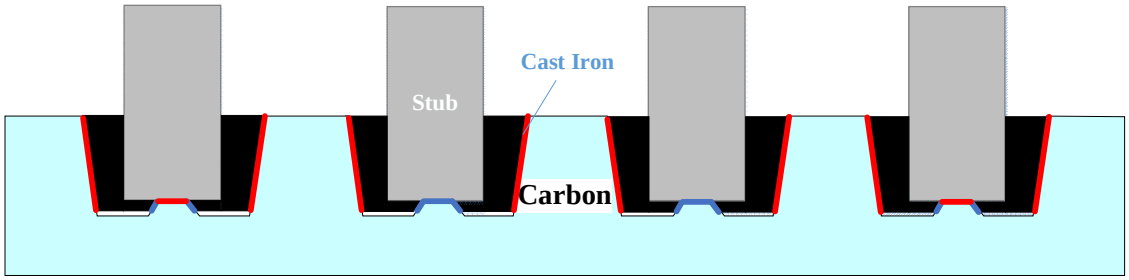

Figure 17. Schematic diagram of contact status in the stub hole of Case 6.

Compared with the conventional anode (Case 1), the contact interfaces area increased by 1.3 %, to 0.43261 m^2. The total anode voltage drop is 363.0 mV in this situation. Here, because of the contact area is much smaller, the saving is also smaller, about 2.3 mV.

3.7. Summary

Based on the thermal-electrical simulation results, the estimated voltage drop saving ranges from 2.3 mV to 5.6 mV. The increased contact interfaces area is an important factor which leads to the reductions in total anode voltage drop. Comparing with Case 1, Case 2 has a voltage drop reduction of 5.6 mV because there are 8 more pairs of contact interfaces bringing 6 % more contact area in total. In Case 3, the increased contact area is less than that of Case 2. So even Case 3 can reduce the total anode voltage drop, the reduction is less than that in Case 2. The same situation arises for Case 6

However, sometimes a larger increased contact area cannot lead to a larger voltage drop reduction. Compared with Case 5, both of Case 3 and Case 4 have a lower voltage drop reduction but the larger contact areas. This is because the voltage drop reduction depends not only on the increased contact area, but also on the current distribution. The ideal current

distribution is that the current goes vertically from the top end of the rod to the bottom of the anode. If the top surface of the pin can contact the bottom of stub, the current route would be shortened. As a result, the contact of the top surfaces on the pins are more important than that on their side surfaces.

Table 4. Summary of results.

	Anode voltage drop [mV]	Voltage drop reduction [mV]	Contact area [m^2]	Increased contact area [%]
Case 1	365.3	-	0.42696	-
Case 2	359.7	5.6	0.45249	6.0
Case 3	361.9	3.4	0.44119	3.3
Case 4	360.6	4.7	0.44684	4.7
Case 5	360.6	4.7	0.43827	2.6
Case 6	363.0	2.3	0.43261	1.3

3.8. Estimated Cost Saving

The cost saving of this kind of anode design was estimated with the following data for a smelter: amperage 450 kA, 400 cells, current efficiency 94 % and energy cost 40 $/MWh. The metal production of the smelter is 497 384 tonnes per year. In this paper, we calculated the voltage saving of approximately from 2.3 to 5.6 mV. The energy saving is then from 0.0073 to 0.0178 kWh/kg Al or 3626.67 to 8830.15 MWh per year for the smelter. The cost saving is 145 792 $ to 353 206 $ per year.

4. Conclusion

In this paper, a thermo-electrical model has been developed to investigate the effects of a kind of Chinese anode design on anode voltage drop in different situations. This design, where pins are added at the bottom of the stub holes, can increase the contact area from 1.3 % to 6 % and reduces the voltage drop from 2.3 mV to 5.6 mV. Simulation results show also that the contact on the top surfaces of pins is more important than in their side surfaces. This voltage drop improvement would lead to an annual cost saving estimated from 145 792 $ to 353 206 $ per year for a smelter producing 499 871 tonnes of aluminium if the energy cost is 40 $/MWh. However, for a better characterization of this design, more simulations must be done, especially with the coupling between thermo-electrical and mechanical fields.

5. Acknowledgement

The first author acknowledges the financial support from the Chinese Scholarship Council (CSC). The authors would like to acknowledge the National Sciences and Engineering Research Council of Canada (NSERC) funding NSERC Discovery Grant (No. 36518), the Fundamental Research Funds for the Central Universities (Grant No. N162503004, N162502002), China

Postdoctoral Science Foundation (Grant No.2017M610183), the National Natural Science Foundation of China (Grant No. 51228401, 51529401, 51434005, 51574070, 51474060), the National Key Technology Research and Development Program of the Ministry of Science and Technology of China (Grant No. 2012BAE08B01) for supporting the present research. A part of the research presented in this paper was financed by the Fonds de Recherche du Québec-Nature et Technologie (FRQNT) by the intermediary of the Aluminium Research Centre-REGAL.

6. References

1. Qiu Zhu-xian. Aluminium metallurgy of Prebaked Anode Reduction Cells, *Metallurgical Industry Press*, 2005.
2. Z. Tsomaev, Anode for the electrolysis of aluminium: *U.S. Patent Application* 10/250,627, 2002-1-14.
3. M. Fafard, O. Trempe, P. Goulet et al., Anode and Connector for a Hall-Heroult Industrial Cell, WO, WO/2012/100340, 2012.
4. S.O. Tremblay, D. Marceau, D. Kocaefe et al., Development of a New Approach to Increase the Electrical Performance of Anodic Assemblies, *Light Metals* 2015, 1175-1180.
5. Zhao Hongjun, Energy Saving Effects of the Technology Slotting between the Adjacent Stub-Hole on Prebaked Anode Carbon Block, *Journal of Materials and Metallurgy*, 2010 (S1), 92-94.
6. Hu Kaihua, He Xinguang, Chen Yanling et al., Low Consumption Prebaked anode for Aluminium electrolysis, CN104498997A. 2015.
7. H. Chaouki, M. Baiteche, A. Jacques et al., Finite Element Analysis of Slot Size Effect on the Thermal-Electrical Behaviour of the Anode, *Light Metals* 2017, 1315-1323.
8. D. Richard, P. Goulet, O. Trempe et al., Challenges in Stub Hole Optimisation of Cast Iron rodded Anodes, *Light Metals* 2009, 543-548.
9. D.R. Gunasegaram, D. Molenaar, Towards improved energy efficiency in the electrical connections of Hall–Héroult cells through Finite Element Analysis (FEA) modeling. *Journal of Cleaner Production*, 2015, 93, 174-192.
10. H. Fortin, N. Kandev, M. Fafard, FEM analysis of voltage drop in the anode connector induced by steel stub diameter reduction, *Finite elements in analysis and design*, 2012, 52, 71-82.
11. Mohamed I Hassan, Ayoola Brimmo, Rawa Ba Raheem et al., Validation of Anode Model for Voltage Drop Mitigation Studies, *34th International Symposium ICSOBA*, Quebec, Canada, October 2016, *Travaux*, No. 45, 2016, Paper AL 36, 847-859.